



## Research papers

## Influence of urban forms on surface flow in urban pluvial flooding

Martin Bruwier<sup>a</sup>, Claire Maravat<sup>a,b</sup>, Ahmed Mustafa<sup>c</sup>, Jacques Teller<sup>d</sup>, Michel Piroton<sup>a</sup>, Sébastien Erpicum<sup>a</sup>, Pierre Archambeau<sup>a</sup>, Benjamin Dewals<sup>a,\*</sup>

<sup>a</sup>Hydraulics in Environmental and Civil Engineering (HECE), Urban & Environmental Engineering (UEE), University of Liege, Liege, Belgium

<sup>b</sup>Université de Montpellier, France

<sup>c</sup>Urban Systems Lab, The New School, New York, NY, USA

<sup>d</sup>Local Environment Modelling and Analysis (LEMA), Urban & Environmental Engineering (UEE), University of Liege, Liege, Belgium

## ARTICLE INFO

This manuscript was handled by G. Syme, Editor-in-Chief, with the assistance of Xiaodong Zhang, Associate Editor

## Keywords:

Urban pluvial flood  
Porosity shallow-water model  
Procedural modelling

## ABSTRACT

This paper presents a systematic analysis of the influence of nine urban characteristics (distance between buildings, mean building size, building coverage, etc.) on surface flow in case of pluvial flooding. Time dependent stored volumes, outflow discharges and mean water depths were computed for a set of 2000 synthetic urban forms, considering various terrain slopes and return periods of the rainfall. An efficient porosity-based surface flow model was used to compute the 2D flow variables. Statistical analysis of the relationship between the flow and urban variables highlights that the flooding severity is mostly influenced by the building coverage.

## 1. Introduction

Worldwide, urban flooding induces a broad range of damage to people, infrastructure and economy (e.g. Huang et al., 2017; Yin et al., 2016; Kreibich et al., 2019). Urban flood risk is growing as a result of rapid urbanization and increasingly frequent hydroclimatic extremes (Zhou et al., 2012; Chen et al., 2015; Muis et al., 2015; Yin et al., 2015; Miller and Hutchins, 2017). A major cause of flooding in inland urban areas is pluvial floods, induced by heavy rainfall events (Gaines, 2016). Existing research on urban pluvial flooding has covered a broad range of aspects, including spatio-temporal precipitation data, rainfall-runoff modelling, risk management and impact analysis of climate and land-use change.

## 1.1. Existing data and models

Hydrological modelling of urban catchments remains particularly challenging due to (i) limitations in data availability, (ii) specific flow processes such as the interactions between surface flow and urban drainage systems, (iii) as well as the spatial heterogeneity of urban features influencing runoff (Leandro et al., 2009; Salvatore et al., 2015).

In early studies, the urban surface water runoff originating from point sources, such as manholes, has been simulated with 2D surface

flow routing models, either based on the full 2D shallow-water equations (Mignot et al., 2006; Martins et al., 2017) or on simplified versions such as inertial formulation (e.g. Fewtrell et al., 2011).

Other research applied sequentially a 1D model for the urban drainage system and a 2D model for surface flow routing. The outcome of the urban drainage model consists in hydrographs of surcharged flow (i.e. excess flow compared to the design discharge of each pipe section), used as an input for the 2D surface flow routing model. Based on this approach and a 2D diffusive surface flow model, Hsu et al. (2000) simulated inundation in urban areas caused by the surcharge of storm sewers and considering the influence of pumping stations. Nonetheless, even in this approach, two-way interactions between the surface flow and the urban drainage system are not reproduced explicitly.

In contrast, *dual-drainage* modelling consists in coupling a 1D flow routing model for the urban drainage system and a 2D surface flow routing model (Schmitt et al., 2004; Djordjević et al., 2005; Chen et al., 2007; Seyoum et al., 2012; Löwe et al., 2017). The bidirectional interactions between the two models are ensured through sink and source terms in the respective model equations. These terms are evaluated from weir or orifice formulae (Bazin et al., 2014). In so-called *hydro-inundation models*, precipitation is incorporated as a source term in the 2D surface flow routing model and this model contains an explicit representation of hydrological processes such as infiltration (Cea et al., 2010; Yu and Coulthard, 2015; Leandro et al., 2016; Löwe et al., 2017)

\* Corresponding author.

E-mail addresses: [mbruwier@uliege.be](mailto:mbruwier@uliege.be) (M. Bruwier), [claire.maravat@orange.fr](mailto:claire.maravat@orange.fr) (C. Maravat), [a.mustafa@newschool.edu](mailto:a.mustafa@newschool.edu) (A. Mustafa), [jacques.teller@uliege.be](mailto:jacques.teller@uliege.be) (J. Teller), [michel.piroton@uliege.be](mailto:michel.piroton@uliege.be) (M. Piroton), [s.ericum@uliege.be](mailto:s.ericum@uliege.be) (S. Erpicum), [pierre.archambeau@uliege.be](mailto:pierre.archambeau@uliege.be) (P. Archambeau), [b.dewals@uliege.be](mailto:b.dewals@uliege.be) (B. Dewals).

<https://doi.org/10.1016/j.jhydrol.2019.124493>

Received 9 May 2019; Received in revised form 30 October 2019; Accepted 17 December 2019

Available online 19 December 2019

0022-1694/ © 2019 Elsevier B.V. All rights reserved.

and evaporation (Yu and Coulthard, 2015; Yin et al., 2016, 2019), to replace the total rainfall by the effective rainfall. While in conventional approaches catchment modelling and floodplain modelling are two successive steps, in hydro-inundation models they are merged into a single computation. In several studies, dual-drainage and hydro-inundation features were combined (Hsu et al., 2000; Schmitt et al., 2004; Leandro et al., 2016). In contrast, others opted for a simplified description of the urban drainage system, such as assuming that water is drained away at the design capacity, without explicit representation of drains and manholes (Yu and Coulthard, 2015; Yin et al., 2016, 2019), or even neglected the urban drainage system (Huang et al., 2017). In existing dual-drainage and hydro-inundation models so far, the surface flow was represented using non-inertia 2D flow models.

The broad range of developed models has proved valuable to support urban flood risk management as well as for the planning and management of urban drainage systems (Fletcher et al., 2013). They have been used in various settings, including for evaluating the impact of flooding on traffic disruption (Yu and Coulthard, 2015; Yin et al., 2016, 2019), for urban flood forecasting (Chen et al., 2015), for assessing pluvial flood risk at the local level (Elboshy et al., 2019), among other applications.

### 1.2. Influence of urban planning on urban pluvial flooding

Many recent studies have investigated the sustainable management of urban storm water based on Low Impact Development (LID) techniques (i.e. seeking to mimic a site's pre-development hydrology), such as tanks, swale, green roof or permeable pavement (Qin et al., 2013; Ahiablame and Shakya, 2016; Chen et al., 2017). Others analysed the impacts of urbanization on urban pluvial flooding. For instance, based on a hydro-inundation model, Huang et al. (2017) and Miller and Hutchins (2017) highlighted that land-use and land cover changes substantially contribute to increase pluvial flooding in urban areas, especially for extreme rainfall events.

However, a more limited attention has been paid so far to the specific influence of urban planning policies on urban pluvial flooding. In this regard, only a study carried out by Löwe et al. (2017) stands out. For an urban catchment of 300 ha in Australia, they coupled a 1D-2D hydrodynamic model with an urban development model. They tested nine different urban development scenarios, characterized by contrasting levels of demand for housing, type and location of buildings (uncontrolled urban sprawl involving detached single-unit houses vs. more compact urban forms with multi-storey buildings and apartment blocks) as well as flood adaptation options (buyback of properties, rainwater harvesting, increased stormwater pipe capacity). Their results suggest that, compared to the increase of urban drainage capacity, urban planning policies are more efficient to reduce flood risk under various climate change scenarios.

Nonetheless, even Löwe et al. (2017) paid only limited attention to the role played by the urban form on the severity of urban pluvial flooding, whereas geometry and arrangement of buildings alter the surface flow preferential directions as they represent obstacles to the flow (Leandro et al., 2016). Additionally, existing research focused on individual real-world case studies, and not on more generic configurations; and previous analyses remained generally at the level of the land-use category (e.g. residential, industrial vs. green space), not at the building level.

Therefore, in this paper, we aim to understand whether the geometric characteristics of the arrangement of buildings (also called *urban pattern*) influence surface flow during urban pluvial flooding. More specifically, using regression and correlation analyses, we have been searching for possible relationships between indicators of the severity of urban flooding (stored volume, inundation depth, outflow discharge) and geometric parameters characterizing the urban patterns (typical street width, length, curvature and orientation, building size and distances between buildings).

To do so, we performed a systematic analysis by considering 2000 synthetic, but realistic, urban forms, obtained from a procedural urban generation model. For each of them, we computed the surface flow variables corresponding to three different design rainfalls (15-, 50- and 100-year return periods). The terrain slope was also varied, resulting in a total of 12,000 distinct simulations. This analysis is an extension of the procedure recently developed by (Bruwier et al., 2018) for the case of river flooding.

To perform the high number of necessary model runs, we used an efficient hydro-inundation model developed in-house. It is based on a validated integral porosity shallow-water model solving the fully dynamic shallow-water equations for surface flow (Bruwier et al., 2017a). A simplified approach is used to represent the urban drainage system, which is deemed justified here since the focus is set on comparing the influence on surface flow of the geometric parameters characterizing the urban patterns.

The methodology, detailed in Section 2, includes the generation of synthetic urban forms with a procedural model (Section 2.1), a brief presentation of the hydro-inundation model (Section 2.2) and the statistical approach used to determine the impact of urban parameters on pluvial flow (Section 2.3). Computed flow variables and their relationships with the urban characteristics are presented and discussed in Section 3. Conclusions are drawn in Section 4.

## 2. Methodology

The methodology for evaluating the influence of the urban forms on urban pluvial flooding consists of a chain of two modelling steps and one statistical analysis step, as sketched in Fig. 1. Each step is detailed in the following sections:

- Section 2.1 presents the generation of 2000 synthetic urban forms by means of procedural modelling;
- Section 2.2 describes the computation of surface flow using a porosity-based shallow-water model and design storms of various return periods;
- Section 2.3 details the statistical analysis developed to assess the influence of each urban parameter on the peak values of stored volume, outflow discharge and mean water depth.

### 2.1. Procedural modelling

Synthetic urban forms were generated using a deterministic *procedural modelling* system presented by Mustafa et al. (2018). It consists of a set of rules which enable defining the street network and the arrangement of parcels and buildings based on a limited number of input parameters. The outputs of this urban procedural modelling are collections of locations and footprint geometries of buildings over a pre-defined area. In this study, we considered a square area of 1 km by 1 km and we generated 2000 distinct urban forms by randomly selecting the values of the input parameters.

The input parameters are listed in Table 1. They are identical to those used by Bruwier et al. (2018). The procedural model operates in three steps:

- The network of streets is made of two perpendicular “major” streets and a number of “minor” streets. The skeleton of the network of streets is controlled by parameters  $x_1$  to  $x_3$ . Parameter  $x_1$  defines the typical distance in-between street intersections. The street orientation is controlled by parameter  $x_2 = |\sin [2(\alpha - \pi/4)]|$ , with  $\alpha$  the angle between the west-east direction and the alignment of one of the two main streets. The curvature of the streets is given by  $x_3$  (reciprocal of the typical radius of curvature).
- Parameters  $x_4$  to  $x_6$  influence the number and location of the individual parcels.
- The size and location of the buildings within each parcel are

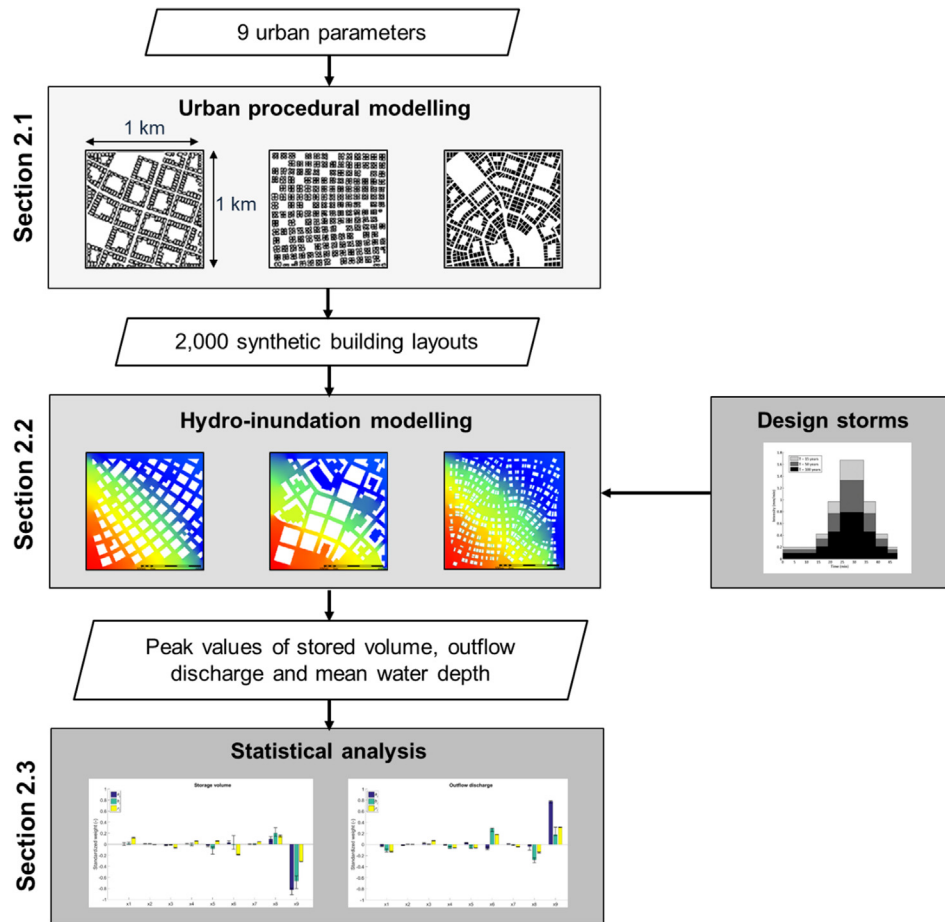


Fig. 1. Methodology involving procedural modelling, hydro-inundation modelling and statistical analysis.

**Table 1**  
Input parameters characterising the synthetic urban forms, and ranges of variation.

	Urban variable	Minimum	Maximum
$x_1$	Average street length	40 m	400 m
$x_2$	Street orientation	0	1
$x_3$	Street curvature	0 km <sup>-1</sup>	10 km <sup>-1</sup>
$x_4$	Major street width	18 m	38 m
$x_5$	Minor street width	10 m	21 m
$x_6$	Mean parcel area	350 m <sup>2</sup>	1100 m <sup>2</sup>
$x_7$	Building rear setback	1 m	5 m
$x_8$	Building side setback	1 m	5 m
$x_9$	Building coverage	0%	43%

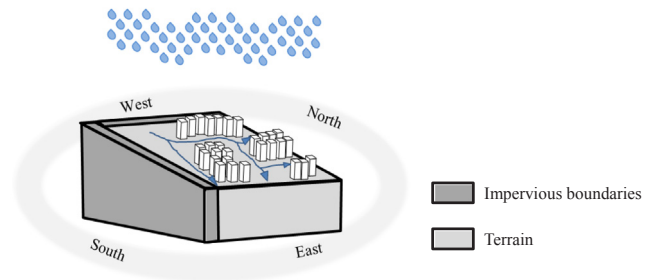


Fig. 2. Schematic representation of the considered 1 km by 1 km urban district on a terrain of uniform slope, with building footprints.

governed by the setbacks  $x_7$  and  $x_8$ , which represent distances between buildings and the borders of the parcels. The building coverage  $x_9$  is the fraction of the total area occupied by buildings. It controls the number of parcels kept without building (i.e. open space).

As shown in Table 1, each input parameter was restricted to a range of variation defined to ensure a sufficient degree of realism of the generated urban forms. These ranges of variation were derived from a sample of real-world cadastral data from Belgium. Nonetheless, the procedural model can also represent a broad range of other urban forms, especially for European cities, as shown by Mustafa et al. (2018).

A complete description the flow process of the procedural model is given by Bruwier et al. (2018). Examples of generated urban forms are shown in Fig. 8 hereafter, as well as in Bruwier et al. (2017a, 2018) and Mustafa et al. (2018).

To perform flow computations, the building footprints generated by procedural modelling are placed on an idealized terrain of uniform slope along the direction south-west (highest level) to north-east (lowest level) (Fig. 2). Two distinct slopes were tested: 1.4% and 2.8%. Idealizing the topography as a plane is a strong assumption; but it is motivated by our intention to focus here our systematic analysis on the influence of the urban forms. Therefore, we did not want to include additional independent variables characterizing a more complex topography (e.g. location, extent, depth of sinks...).

### 2.2. Hydro-inundation model

For each of the 2000 synthetic urban forms introduced in Section 2.1, surface flows occurring during urban pluvial flooding were computed under identical flow boundary conditions and hydrological

forcing (design storms).

To perform the flow computation, we used an existing porosity-based shallow-water model. Such porosity-based models enable using relatively coarse computational cells while preserving to some extent the detailed topographic information at a subgrid-scale by means of storage and conveyance porosity parameters (Sanders et al., 2008). This approach enables speed-up factors of the order of  $10^2$  to  $10^3$  compared to standard shallow-water models, while keeping a similar level of accuracy (Guinot et al., 2017). This made the systematic analysis of 2000 urban forms tractable.

We applied here the same porosity-based model as used by Bruwier et al. (2018) for assessing the influence of the urban forms in the case of river flooding. The model was introduced and extensively validated by Bruwier et al. (2017a). It was also repeatedly applied for modelling urban flooding (Arrault et al., 2016; Bruwier et al., 2017b, 2018). An additional piece of validation against experimental observations is provided in Supplementary material A for flow conditions corresponding specifically to pluvial flooding.

The flow computations were performed using a Cartesian grid with a spacing  $\Delta x = 10$  m, a Manning roughness coefficient  $n = 0.01 \text{ sm}^{-1/3}$ , a drag coefficient  $c_D = 2$  and a minimum threshold porosity  $\phi_{\min} = 0.1$ . The influence of these parameters, particularly the grid size, was tested by Bruwier et al. (2017a) for geometric configurations (urban forms) identical to those considered here.

As sketched in Fig. 2, impervious upstream boundaries were prescribed along the south and west sides of the urban district, while a rating curve was prescribed as a downstream boundary condition along the north and east sides. This rating curve is a lumped representation of the flow conditions further downstream of the urban area under study. It relates the local runoff unit discharge to the power 3/2 of the runoff depth (Bruwier et al., 2018). The buildings are represented as impervious blocks.

The specific objective of the present study is not to represent a given real-world flooding event, but instead to conduct a comparative analysis of the influence of urban characteristics on surface flow during urban pluvial flooding. Therefore, the selection of the rainfall input is to a great extent arbitrary, provided that it remains representative of real situations. We opted for three distinct design storms corresponding to return periods of 15, 50 and 100 years in a Belgian municipality (Hosseinzadehtalaei et al., 2018). This range of return periods is consistent with that used in other similar researches (Yin et al., 2016; Huang et al., 2017). More details on the design storms are given in Supplementary material B.

The model accounts for direct rainfall input but it does not represent the urban drainage explicitly. While in some studies the urban drainage system was assumed overwhelmed and therefore simply neglected (Mignot et al., 2006; Fewtrell et al., 2011), we opted here for a lumped representation of the urban drainage (e.g. Yu and Coulthard, 2015) by subtracting a portion of the rainfall input (e.g. Skougaard Kaspersen et al., 2017). Consistently with JBA Consulting (2016), we subtracted from the considered design storm the design storm corresponding to a plausible return period taken into account for the sizing of urban drainage systems. This return period was assumed equal to two years. This simplified approach, assuming that the drainage system drains at its design capacity, makes the model more suitable for events strongly dominated by direct surface runoff.

In principle, the spatially distributed effect of drains could be incorporated in the hydro-inundation model; but it was deemed inconsistent with the primary objective of the study, which focuses solely on the influence of the geometry and arrangement of the buildings. Accounting for spatially distributed drains would have required additional arbitrary assumptions (on their location, pipe sizing, network topology ...) which could affect our conclusions.

In previous studies of urban pluvial flooding, infiltration was either neglected (Brown et al., 2007; Chen et al., 2007; Sampson et al., 2013), replaced by an initial abstraction (Chang et al., 2015; Russo et al.,

2015) or computed explicitly by means of dedicated equations such as Green–Ampt (Yu and Coulthard, 2015; Leandro et al., 2016; Yin et al., 2016), Horton (Fernández-Pato et al., 2016; Löwe et al., 2017), or a simplification of the former equations (Skougaard Kaspersen et al., 2017). Here, to avoid extra arbitrary assumptions and keep the focus on the primary aim of this exploratory study, all spaces not occupied by buildings were assumed impervious. The cumulative effects of the urban form and green (infiltration) spaces should be analysed separately. Note that, although disregarding the infiltration in green areas is a strong assumption, adding infiltration processes in the present systematic analysis of a broad range of urban forms would dramatically increase the number of independent variables (spatial distribution, extent and infiltration capacity of green areas), which in turn would make the conclusions less focused on the “effects of urban forms”.

Evapotranspiration could safely be neglected due to the urban nature of the catchment and the relatively short time scales of interest here (Yu and Coulthard, 2015).

Another common challenge in the modelling of urban pluvial flooding relates to the impact of the building roofs on the rainfall–runoff processes, mainly due to a general lack of knowledge on the roofs drainage structure. By introducing a constant user-defined routing velocity for shallow areas (including the roofs of the buildings), Sampson et al. (2013) conducted stable simulations of direct precipitation onto topography where buildings are present, without requiring prior knowledge or roof drainage structures. Chang et al. (2015) utilised some sub-catchments feature of their model to represent the buildings rainfall–runoff processes. Similarly, Leandro and Martins (2016) set up a conceptual model to reproduce drainage of the rainfall falling on the buildings roofs.

In this study, we opted for a simple conceptual approach, in which we assume that, at every time step, the total amount of rainfall falling on the roof of a given building is drained instantaneously and transferred to the surface flow computation in the cells corresponding to the vertices of the building footprint contour. The rainfall volume reaching a roof over one time step is distributed between the building contour vertices according to the sum of the lengths of the building facades connected to each corner (Fig. 3):

$$d_{i,j}(t) = I(t)\Omega \frac{L_k + L_{k+1}}{2} \left( \sum_{m=1}^M L_m \right)^{-1}, \quad (1)$$

with  $d_{i,j}$  the contribution to the source term in the flow continuity equation due to vertex  $k$  of the considered building,  $I(t)$  the rainfall intensity at time  $t$ ,  $\Omega$  the footprint area of the considered building,  $L_k$  and  $L_{k+1}$  the lengths of the building facades connected to vertex  $k$  and  $M$  the total number of vertices in the contour of the considered building.

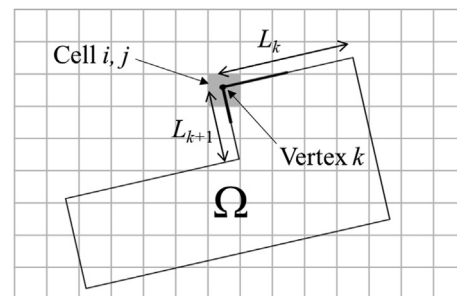


Fig. 3. Sketch of a building footprint represented on the Cartesian computational grid (cells  $i, j$ ), with  $\Omega$  the building footprint area,  $k$  a vertex of the building contour and  $L_k, L_{k+1}$  the lengths of the building facades adjacent to vertex  $k$ .

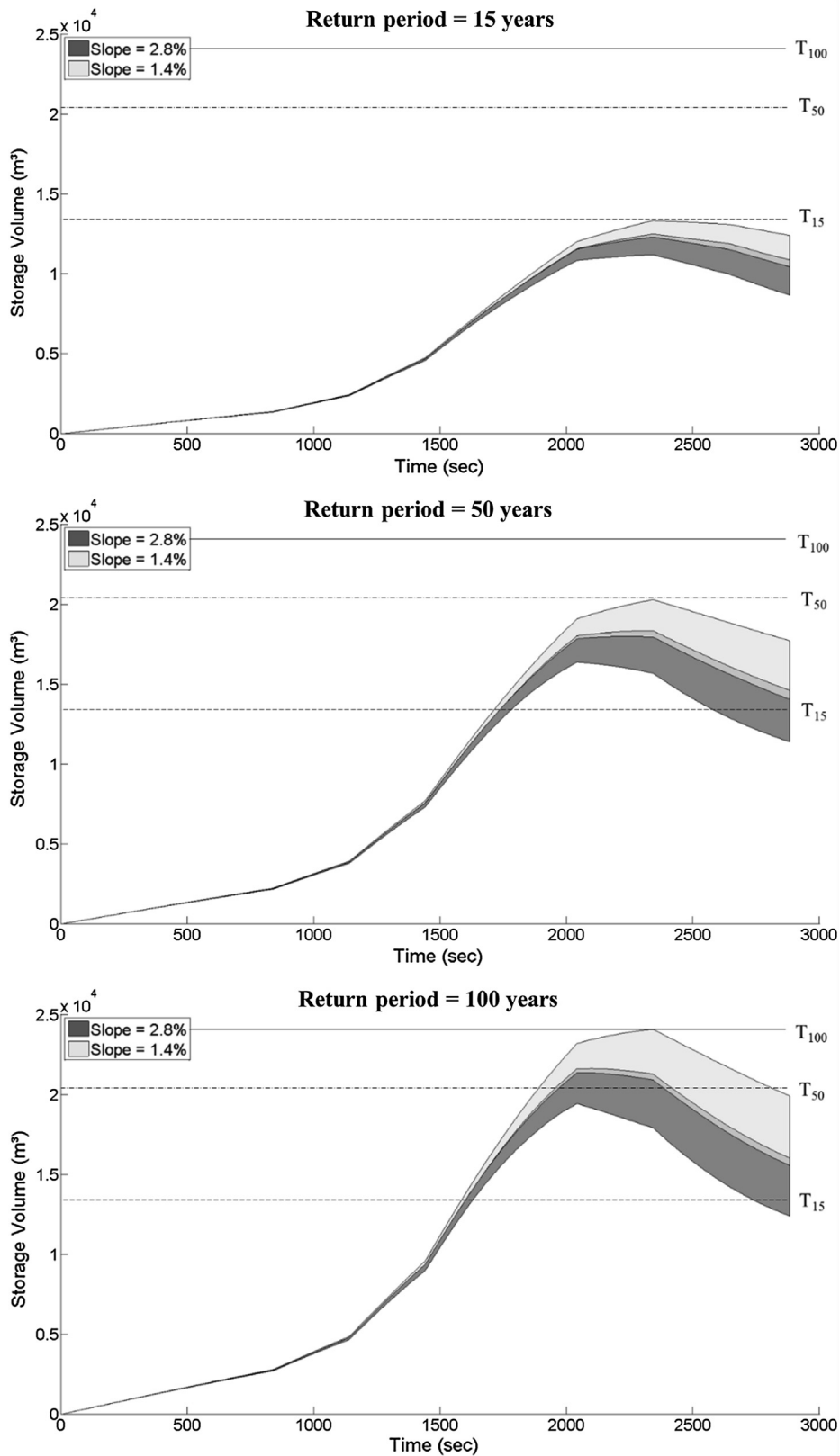


Fig. 4. Time evolution of the range of values of the stored volume over the 2000 urban forms. Note that the middle grey area corresponds to the area where the dark and light grey areas overlap.

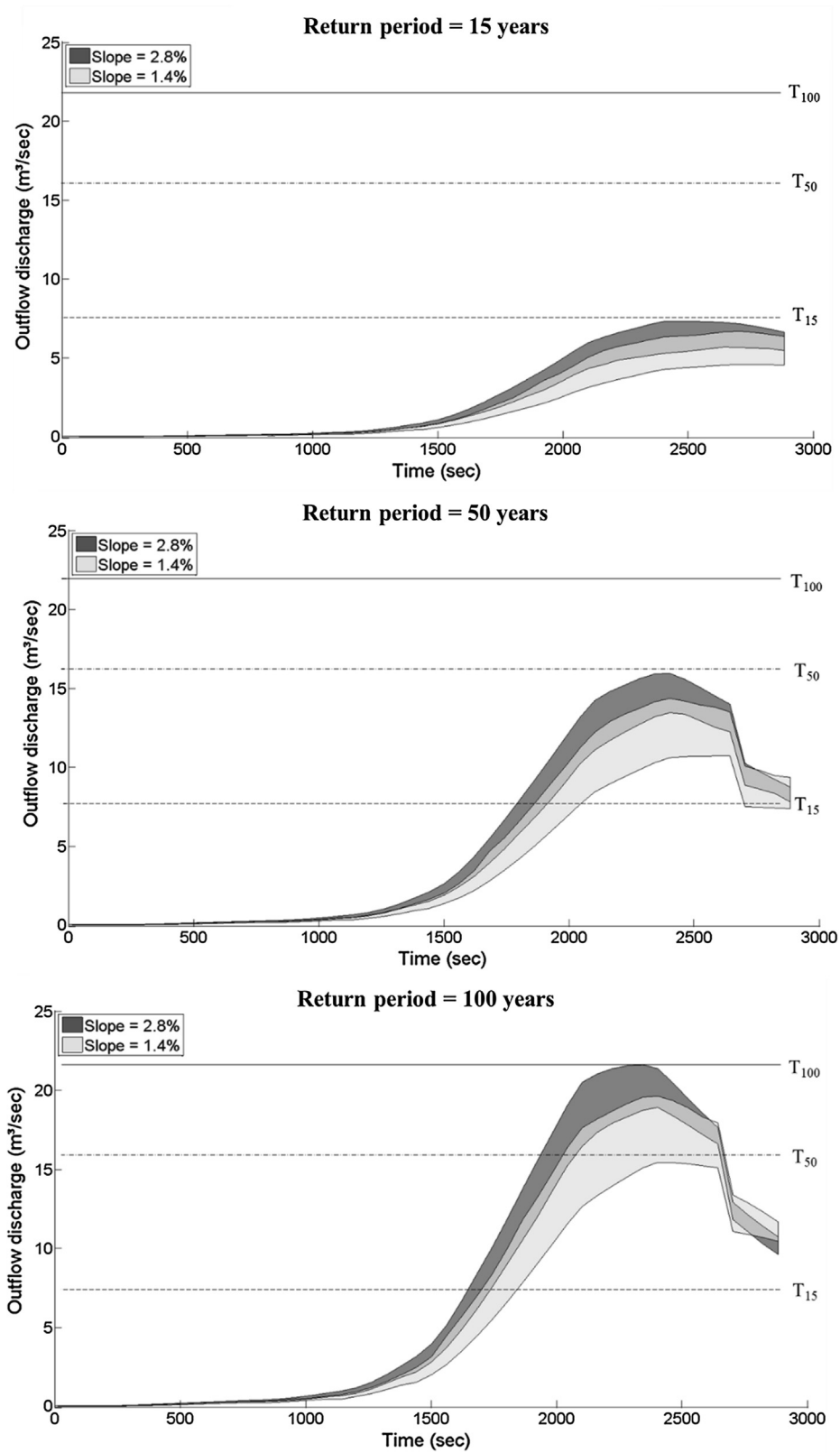


Fig. 5. Time evolution of the range of values of the outflow discharge over the 2000 urban forms. Note that the middle grey area corresponds to the area where the dark and light grey areas overlap.

2.3. Statistical analysis

Three time-dependent flow variables were examined to characterize the severity of urban pluvial flooding:

- the volume of water stored within the urban area ( $V$ ),
- the outflow discharge along the downstream sides ( $Q_{out}$ ), computed as  $Q_{out} = I(t) A - dV/dt$  where  $A$  stands for the total surface of the urban area.

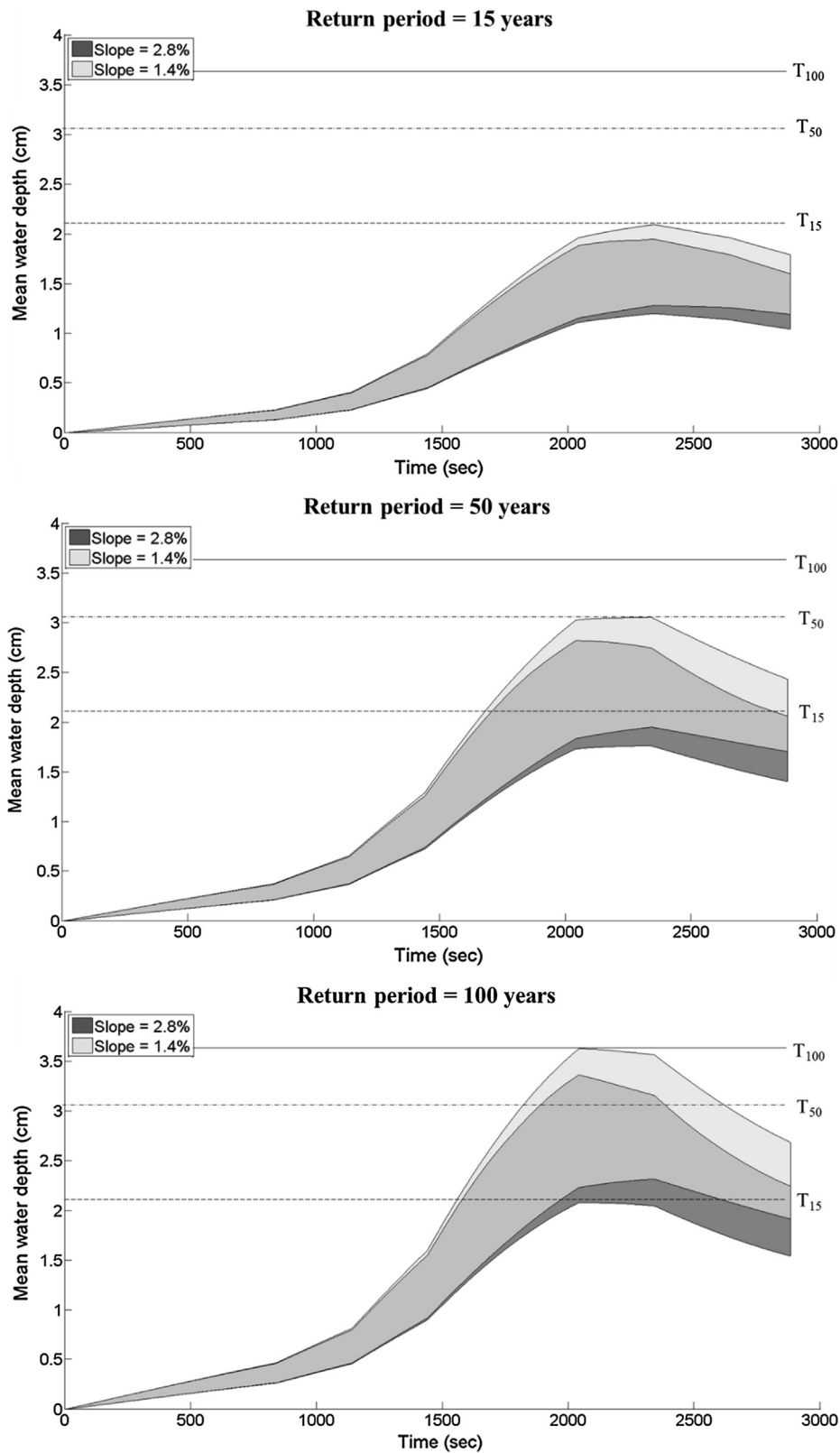


Fig. 6. Time evolution of the range of values of the mean water depth over the 2000 urban forms. Note that the middle grey area corresponds to the area where the dark and light grey areas overlap.

- and the mean water depth ( $h_{\text{mean}}$ ), computed as a spatial-average of the water depth:  $V/A_f$ , where  $A_f$  is the part of the total urban area not occupied by buildings:  $A_f = A (1 - x_9)$ .

For each of these flow variables, a statistical analysis was conducted to highlight possible correlations with the nine urban parameters ( $x_1, \dots, x_9$ ) used as input for procedural modelling (Section 2.1).

The dependent variables considered in the statistical analysis are

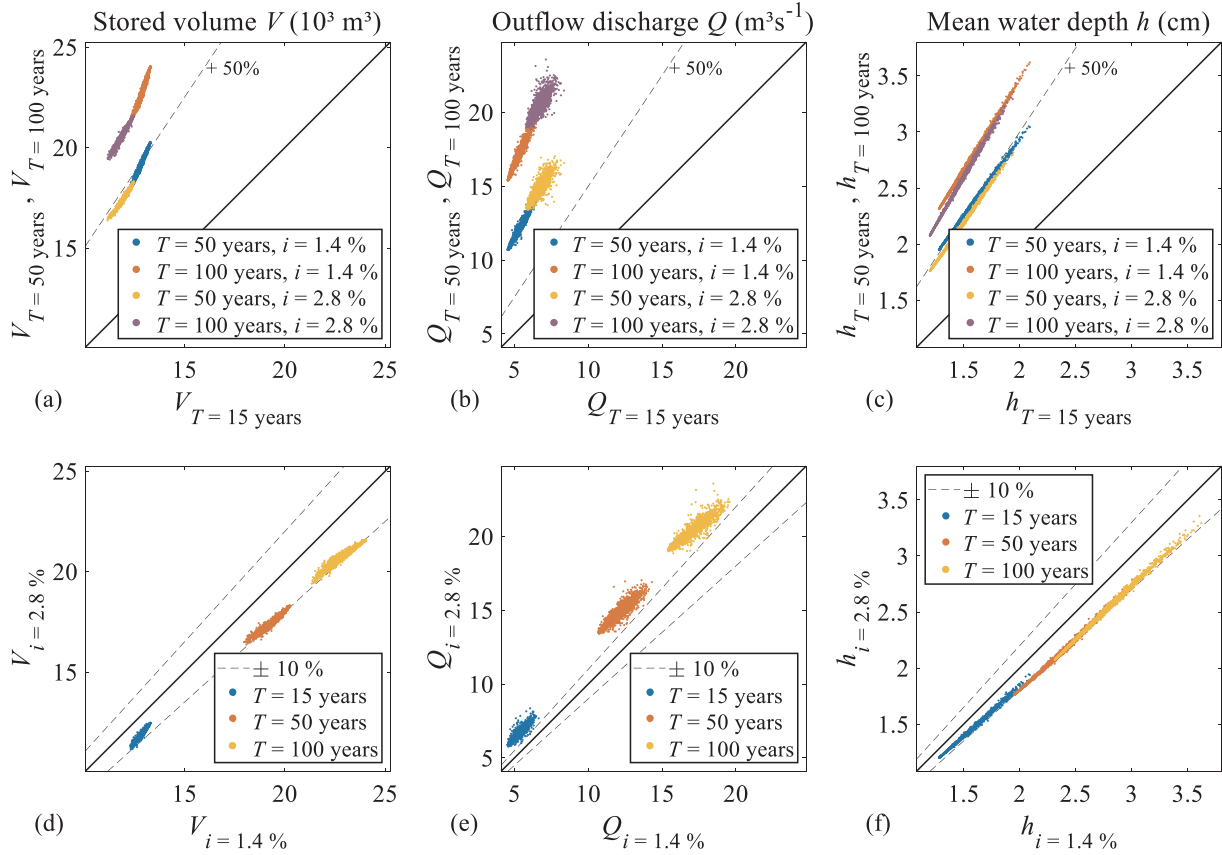


Fig. 7. Scatter plots indicating the influence of the return (a-c) period and the terrain slope (d-f) on the peak values of the flow variables: stored volume (a, d), outflow discharge (b, e) and mean water depth (c, f).

defined as the variation in the peak value of  $V$ ,  $Q_{\text{out}}$  or  $h_{\text{mean}}$  compared to a reference configuration without buildings:

$$y_1 = -([\max_t V]_{\text{test}} - [\max_t V]_{\text{ref}}), \quad (2)$$

$$y_2 = [\max_t Q_{\text{out}}]_{\text{test}} - [\max_t Q_{\text{out}}]_{\text{ref}}, \quad (3)$$

$$y_3 = [\max_t h_{\text{mean}}]_{\text{test}} - [\max_t h_{\text{mean}}]_{\text{ref}}, \quad (4)$$

where subscripts “test” and “ref” refer respectively to any of the 2000 tested urban configurations, and to a reference configuration without buildings. Eq. (2) ensures positive values of  $y_1$  since the peak value is maximum in the absence of buildings (Section 3.2).

To ensure the robustness of the conclusions, we used three distinct approaches for the correlation and regression analyses:

- first, a multiple linear regression (MLE) was applied to standardized variables:

$$\frac{y_j - y_{j,\text{mean}}}{y_{j,\text{std}}} = a_{0,j} + \sum_{i=1}^9 a_{i,j} \frac{x_i - x_{i,\text{mean}}}{x_{i,\text{std}}}, \quad (5)$$

where  $a_{i,j}$  ( $i = 0-9$ ,  $j = 1-3$ ) are the coefficients of the MLR, while the subscripts “mean” and “std” denote respectively the mean and the standard deviation of the corresponding variable over the sample of 2000 urban configurations;

- second, a multiple linear regression was applied to the logarithmic transformation of normalized variables, which is equivalent to:

$$\frac{y_j}{y_{j,\text{mean}}} = b_{0,j} \prod_{i=1}^9 \left( \frac{x_i}{x_{i,\text{mean}}} \right)^{b_{i,j}}, \quad (6)$$

with  $b_{0,j}$  a coefficient and  $b_{i,j}$  the exponents of the normalized explanatory variables  $x_1$  to  $x_9$ ;

- third, Pearson correlation coefficients  $\rho_{ij}$  were computed.

### 3. Results

In the following, we present the results of the flow computation (Section 3.1) and the outcomes of the statistical analysis (Section 3.2). We also discuss which are the most influential urban parameters (Section 3.3).

#### 3.1. Flow variables

We first look at the variation of the flow variables when the urban form is varied, and we compare these variations to those induced by changing the return period of the considered storm or the terrain slope. The envelopes of the time series of stored volume in the urban district, outflow discharge and mean water depth are displayed in Figs. 4–6, respectively. These envelopes reflect the influence of the urban forms on the flow variables. The scatter plots in Fig. 7 summarize the influence of the urban form on the peak values of the three flow variables for the various return periods and terrain slopes. The same information is presented in the form of boxplots in Fig. C.1 in Supplementary material C. The following observations can be made:

- For the three considered flow variables (stored volume, outflow discharge and mean water depth), the width of the envelopes of the time series are not affected by a change in the terrain slope. In contrast, these envelopes become wider when the considered return period is increased (Figs. 4–6). This is also demonstrated by the



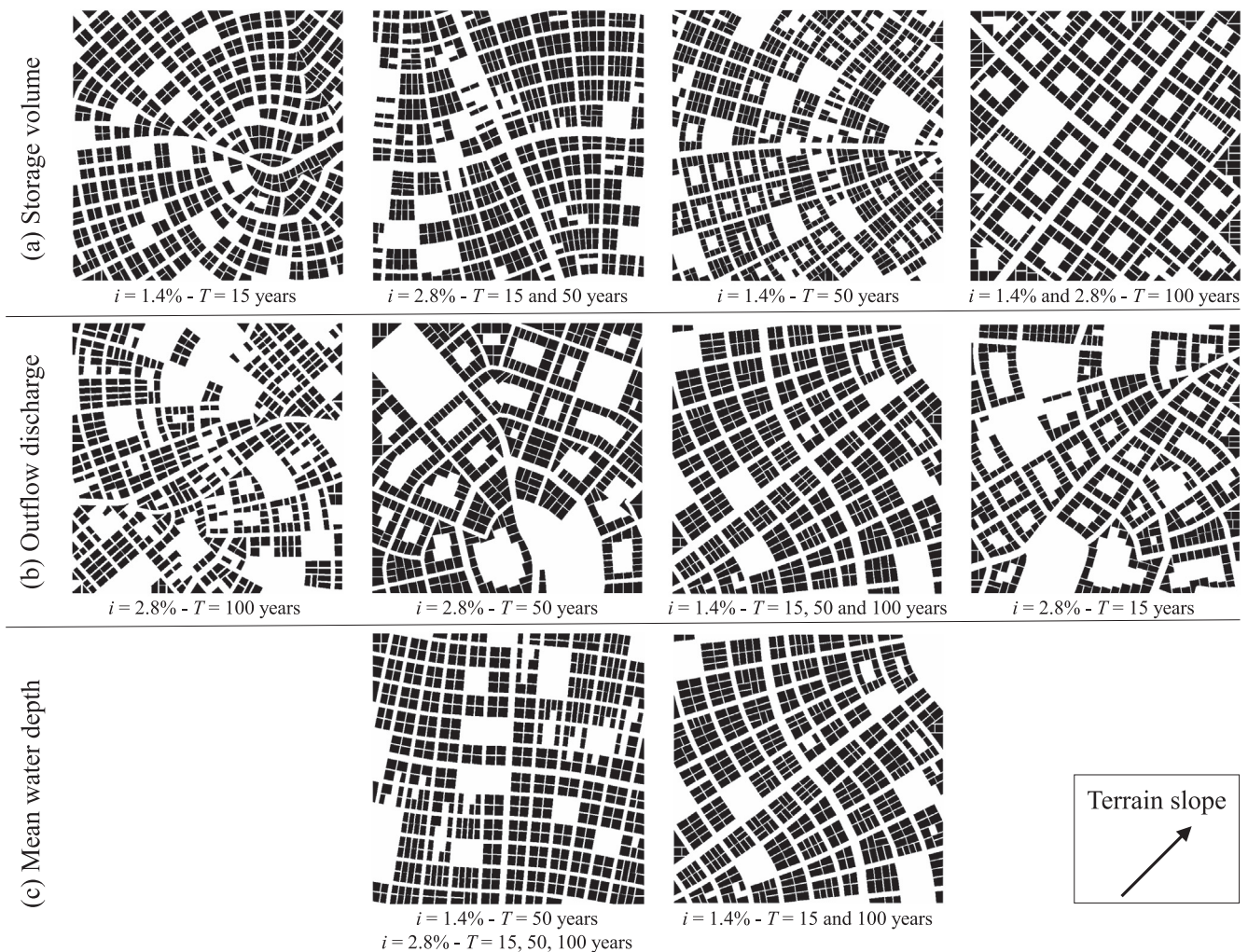


Fig. 8. Building footprints in the urban forms leading to the minimum peak values of the storage volume (a) and maximum peak values of the outflow discharge (b) and mean water depth (c) for the different terrain slopes  $i$  and return periods  $T$ .

scatter plots in Fig. 7a-c, which show a trend with a slope steeper than the 1:1 line, corresponding hence to a wider range of variation along the y-axis (higher return periods) than along the x-axis (lowest return period). This confirms that the influence of the urban form is magnified in the case of more extreme rainfall events. In contrast, when the terrain slope is varied between 1.4% and 2.8%, the range of variation of the flow variables is neither substantially widened nor narrowed (Fig. 7d-f).

- For the three flow variables, the relative influence of the urban form changes over time; and it does so differently depending on the considered flow variable (Figs. 4–6). Indeed, in the case of the stored volume, the width of the envelopes gradually increases with time, whereas for the outflow discharge and mean water depth, the width of the envelope is maximum close to the peak and then it decreases during the recession limb.
- Fig. 4 reveals that the influence of the urban form on the time series of the stored volume in the urban district seems relatively lower than the influence of the terrain slope and of the considered return period. Indeed, this is shown by the fact that the envelopes corresponding to distinct terrain slopes and return periods hardly overlap over the whole rising limb and at the peak of the time series.
- In the case of the outflow discharge (Fig. 5), a limited overlap between the envelopes corresponding to distinct terrain slopes can be seen; but there is still no overlap between the results corresponding to different return periods (see also Fig. C.1 in Supplementary

material C). This suggests that the influence of the urban form is slightly stronger on the outflow discharge than on the time series of stored volume.

- For the peak values of these two flow variables, Fig. 7a-b and d-e show that the ranges of variation corresponding to distinct return periods do not overlap and that the overlaps remain limited when the terrain slope is varied. This highlights that the considered changes in the return period and the tested terrain slopes have a stronger effect on the peak values of stored volume and outflow discharge than variations in the urban form.
- In contrast, for the times series of mean water depths in the urban district (of the order of 0.01–0.04 m), considerable overlaps are found between the envelopes corresponding to distinct terrain slopes and return periods. This points at a relatively stronger influence of the urban form on the mean water depth in the urban district than on the outflow discharge and stored volume. Similarly, substantial overlaps are observed between the ranges of variation of the peaks in water depth when the terrain slope is varied and, to a lesser extent, when the return period is changed (Fig. 7c and f).
- When the return period is increased, the rise in the peak outflow discharges is found twice to three times larger than the rise in the stored volume or in the mean water depth, which change with a similar magnitude, namely +50% between  $T = 15$  years and  $T = 50$  years in the present case (Fig. 7a–c).
- A steeper terrain slope leads to higher peaks in the outflow

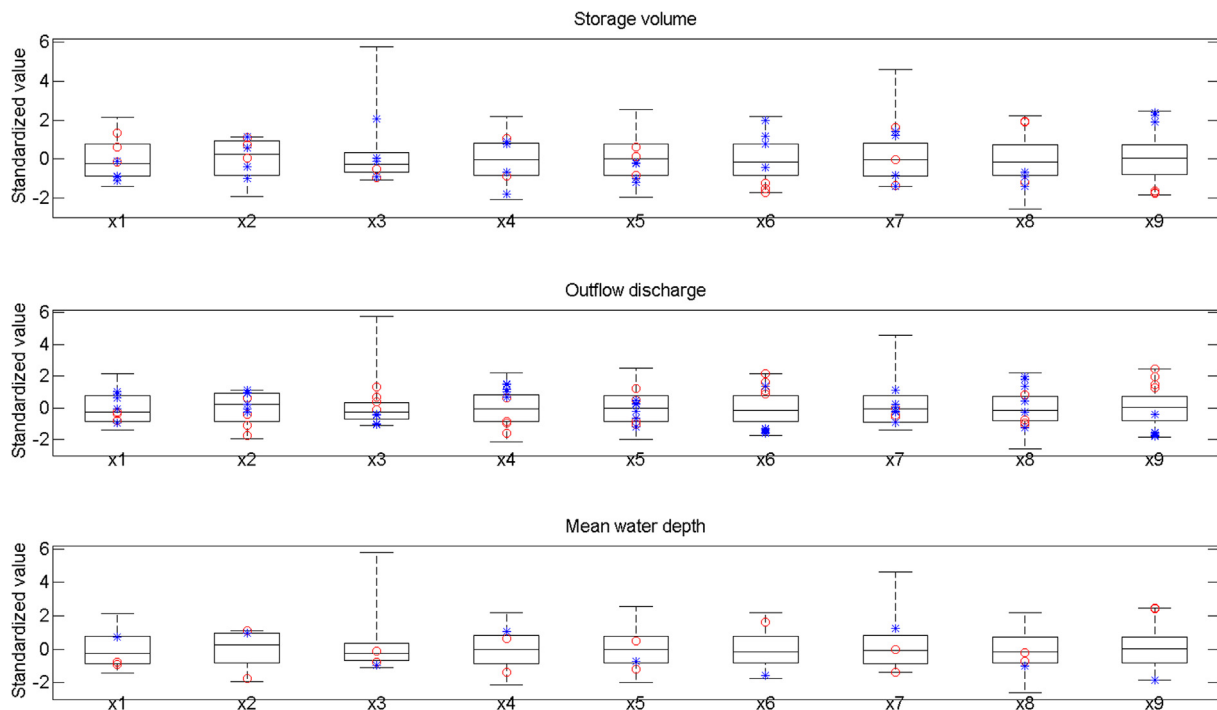


Fig. 9. Standardized values of the nine urban parameters corresponding to urban forms leading to extreme peak values of the three flow variables for the different terrain slopes and return periods (symbols ○: maximum in peak value; symbols \*: minimum in peak value). Boxplots represent the whole set of parameter values over the 2000 urban forms. Note that symbols  $x_1$  to  $x_9$  are defined in Table 1.

discharges and, conversely, lower peaks in the stored volumes and mean water depths (Fig. 7d–f). Again, the peaks in the outflow discharges vary more importantly with the terrain slope than the peaks in the stored volumes and mean water depths ( $-10\%$  in the present case).

- Finally, as clearly visible in the scatter plots in Fig. 7, the results obtained for various return periods and terrain slopes are strongly correlated. Pearson correlation coefficients are, respectively, above 95%, 91% and 99.8% for the stored volumes, the outflow discharges, and the mean water depths. This implies that a more in-depth analysis of the influence of the urban form conducted for a given return period or terrain slope, as performed in the next section, will be essentially transferable to the other return periods and terrain slopes. This statement would certainly not hold if infiltration processes were taken into account by the model.

Note that here the urban forms basically do not influence the timing of the computed peak discharges. However, if both pervious and impervious areas were considered in the simulations, delays would occur in-between the peak discharges depending on where the impervious areas are located.

### 3.2. Influencing urban parameters

Among the 2000 considered urban forms, we identified those which correspond to extreme values in the peaks of the three flow variables (i.e. maximum or minimum values of the peaks in the stored volumes, outflow discharges and mean water depths). This identification was performed independently for the two terrain slopes and the three return periods, but some urban forms lead to extreme peak values in more than one flow variable (Fig. 8).

In Fig. 9, we display the standardized values of the nine urban parameters  $x_i$  (Section 2.1) characterising each of the urban forms leading to a minimum or a maximum in the peak values of the flow variables. Fig. 9 shows also a boxplot representing the whole sets of values of each urban parameter among the 2000 considered urban

forms.

Fig. 9 reveals that none of the urban parameters take consistently an extreme value (high or low) in the configurations leading to extreme peak values in the flow variables; except for parameter  $x_6$  (mean parcel area) and even to a greater extent for parameter  $x_9$  (building coverage) for which this is almost systematically the case. Indeed, maximum peak values of the storage volume (symbols ○ in Fig. 9) and minimum peak values of the outflow discharge and mean water depth (symbols \* in Fig. 9) are consistently associated to low values of the building coverage  $x_9$ . Conversely, minimum peak values of the stored volume (symbols \* in Fig. 9) and maximum peak values of the outflow discharge and mean water depths (symbols ○ in Fig. 9) correspond mainly to high values of the building coverage  $x_9$ . For the outflow discharge, all values of  $x_9$  corresponding to extremes in the peaks of this flow variable lie outside the 25th–75th percentiles interval, at the exception of a single case. For the two other flow variables, there is not a single exception. This hints at an overwhelming influence of the building coverage  $x_9$  in controlling the analysed flow variables during urban pluvial flooding.

The influence of the nine urban parameters on the flow variables was quantified using the statistical approaches presented in Section 2.3. The regression coefficients  $a_i$  and  $b_i$  (respectively without and with logarithmic transform) and the Pearson correlation coefficients  $\rho_i$  are shown in Fig. 10. They were computed using all the results corresponding to the three return periods and the two terrain slopes. Error bars in Fig. 10 indicate the range of variation of the coefficients obtained when individual combinations of return period and terrain slope are considered in the analysis (instead of combining all the configurations). For the outflow discharge and mean water depth, a positive value of a coefficient indicates that increasing the value of the corresponding urban parameter leads to a rise in the peak value of the flow variable. In contrast, a positive coefficient corresponds to an opposite variation in the case of the stored volume. This is due to the definition of the dependent variable  $y_1$ , as detailed in Section 2.3.

The results disclose the following:

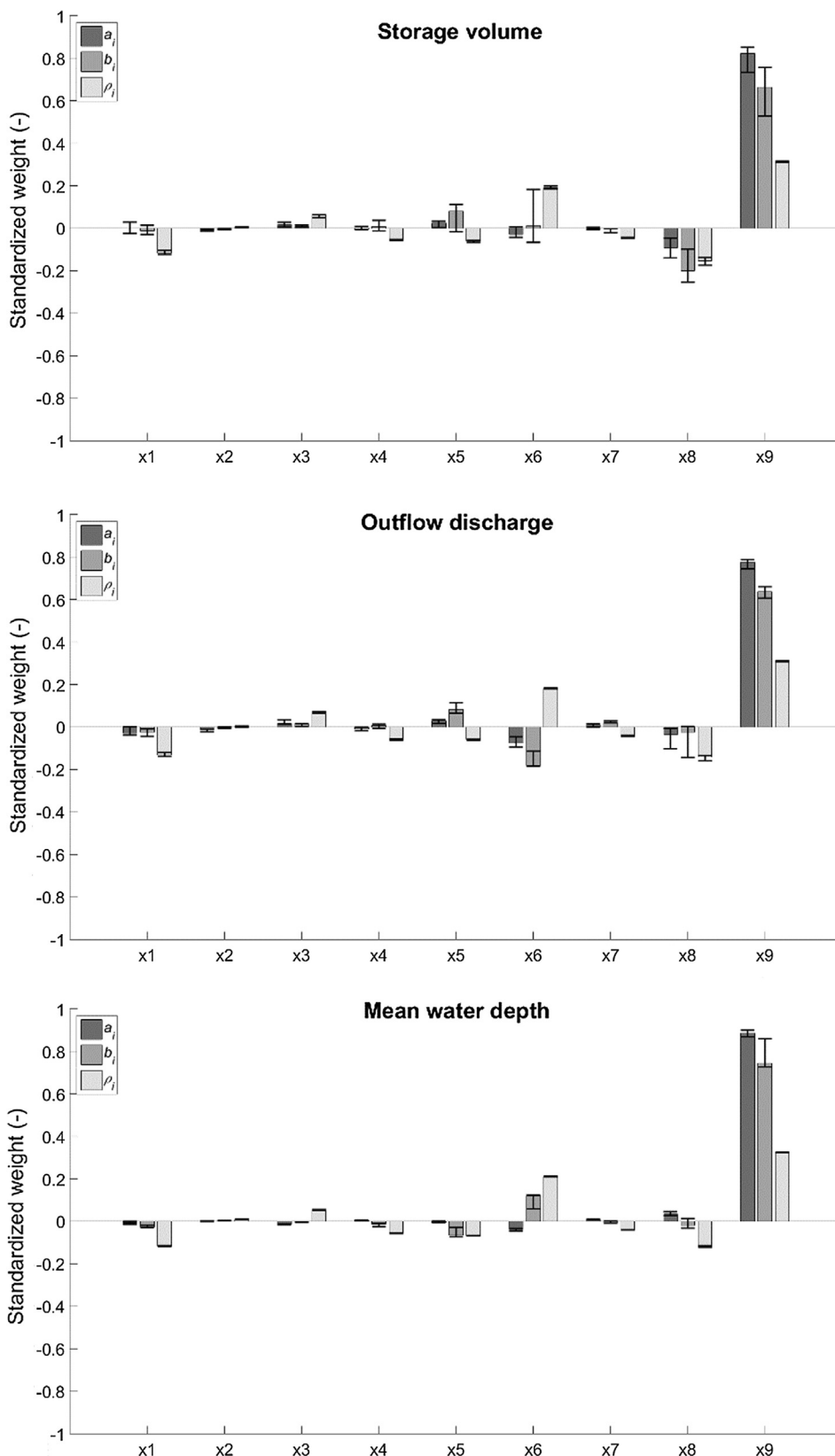


**Fig. 10.** Comparison of regression coefficients  $a_i$  and  $b_i$  obtained from multiple linear regression respectively without and with logarithmic transform, and Pearson correlation coefficients  $\rho_i$  computed from computations over the six combinations of terrain slopes and return periods. Each set of coefficients are standardized so that the sum of the nine absolute values is one. Intervals gives the extreme values obtained for specific combinations of terrain slopes and return periods. Symbols  $x_1$  to  $x_9$  are defined in Table 1.

**Table 2**

Error  $E$  on the predicted value of the peak flow variables using different sets of explanatory urban parameters and two linear regression models. Note that symbols  $x_1$  to  $x_9$  are defined in Table 1.

Urban parameters	Multiple linear regression (MLR): Eq. (5)			MLR with logarithmic transform: Eq. (6)		
	$x_1$ to $x_9$	$x_8$ and $x_9$	$x_9$	$x_1$ to $x_9$	$x_8$ and $x_9$	$x_9$
Stored volume	12.4%	12.6%	13.4%	11.7%	11.9%	13.4%
Outflow discharge	16.2%	17.0%	17.3%	16.1%	16.6%	17.1%
Mean water depth	7.2%	7.4%	7.4%	4.9%	5.0%	5.1%

**Table 3**

Coefficients obtained from a linear regression with logarithmic transform accounting for the urban parameters  $x_8$  and  $x_9$ . Note that symbols  $x_1$  to  $x_9$  are defined in Table 1.

$y_j = b_{0,j}x_8^{b_{8,j}}x_9^{b_{9,j}}$	$b_{8,j}$	$b_{9,j}$
Storage volume	-0.27	0.95
Outflow discharge	-0.19	1.1
Mean water depth	0.034	1.2

- As inferred from previous results, the statistical analysis confirms the dominating influence of the building coverage  $x_9$ , which shows generally the coefficient with the largest magnitude. The corresponding  $p$ -values are all virtually equal to zero, confirming the statistical significance of this result. This means that raising the value of the building coverage reduces the peak value of the stored volume, consequently to a reduction in the void area, and it increases the peak values of the outflow discharges and mean water depths. This result is also highlighted by the scatter plots displayed in Supplementary material D.
- All coefficients associated to the urban parameters  $x_1$  to  $x_5$  and to  $x_7$  remain consistently low in magnitude, revealing a limited influence of these urban parameters on the studied flow variables.
- The variations in the coefficients associated to  $x_6$  (mean parcel area) when the statistical approach is varied are explained by the existing positive correlation between parameters  $x_6$  and  $x_9$ , as detailed in Bruwier et al. (2018). Indeed, when a statistical approach leads to a relatively lower (resp. higher) coefficient for  $x_6$ , it is compensated by a higher (resp. lower) value of the coefficient associated to  $x_9$ .
- Besides the building coverage, the second most influential urban parameter seems to be the lateral setback  $x_8$ , which is closely related to the distance between adjacent buildings. This is particularly true for the stored volume and the outflow discharge. Indeed, increasing the side setback enhances the connectivity between various parts of the urban area, hence enabling more effective storage over the duration of the storm. The corresponding  $p$ -values are generally very close to zero and, at most of the order of  $9 \times 10^{-3}$ .

Overall, these results are to a great extent consistent with those obtained by Bruwier et al. (2018) for river flooding. The main difference is that the dominating influence of the building coverage on the flow variables is more severe for pluvial flooding than for river flooding.

Since the analysis above is based on the mean water depth, it does not reflect explicitly the effect of urban forms on the spatial distribution of water depths. To address this, Supplementary material E looks at the effect of choosing alternate representative water depths (such as various percentiles). The results of the statistical analysis performed based on these alternate representative water depths reveal that the relative influence of the urban parameters remains essentially similar in all cases, so that the above conclusions still apply, particularly as regards

the overwhelming influence of the building coverage ( $x_9$ ).

### 3.3. Number of urban variables used in the statistical analysis

The statistical analysis presented in Section 3.2 highlighted the dominant influence of the building coverage on the peak values of the flow variables compared to a configuration without buildings. Here, we compare the predictive capacity of regression models involving either the nine urban parameters  $x_1$  to  $x_9$  or a subset of them (either the building side setback  $x_8$  and the building coverage  $x_9$ , or only the building coverage  $x_9$ ). The capacity of each regression model to predict the peak value of flow variable  $j$  is evaluated through the error  $E_j$  computed as follows:

$$E_j = \frac{\sum_{i=1}^N |y_{ij} - \tilde{y}_{ij}|}{N y_{j,\text{mean}}} \tag{7}$$

where  $\tilde{y}_{ij}$  is the predicted value of the peak flow variable  $y_j$  corresponding to urban form  $i$ .

As shown in Table 2, the errors are minimum when all urban parameters are taken into account; but the errors increase only marginally if all parameters but  $x_9$ , or  $x_8$  and  $x_9$ , are disregarded. Particularly for peaks in mean water depths, the error hardly changes when the regression model accounts only for  $x_9$ , or  $x_8$  and  $x_9$  (increase in  $E_j$  by maximum 0.2 percentage points). This strengthens the claim that the considered flow variables are essentially controlled by the building coverage and, to a lower extent, by the lateral setbacks.

The results in Table 2 also highlight that, for the three flow variables, the error on the predicted peak values is lower with the logarithmic transform than without. This is consistent with the formulation of Eq. (5) which appears more physically sound than Eq. (6). Also, the peaks in mean water depths are predicted with a better accuracy ( $E_j \approx 5\%$ ) than the peaks in stored volumes ( $E_j \approx 12\text{--}13\%$ ) and in outflow discharges ( $E_j \approx 16\text{--}17\%$ ). Note that the errors are evaluated in the untransformed space.

Table 3 shows the coefficients derived from a multiple linear regression model with logarithmic transform based on urban parameters  $x_8$  and  $x_9$ . The results emphasize the relatively lower influence of the lateral setback  $x_8$  on the peak flow variables. The building coverage has a weight about one to two orders of magnitude larger than the lateral setback for the prediction of the peaks in stored volume, outflow discharge and mean water depth. From the perspective of urban planning, this considerable difference in the weights hampers the compensation of an increased building coverage (i.e. urban development) by a “flood-sensitive” arrangement of the buildings (e.g. with higher lateral setbacks), since the latter effect remains by far smaller than the former one. This contrasts with the case of river flooding

(Bruwier et al., 2018), where the relative influence of the building coverage and another composite indicator of the buildings arrangement differs only by a factor three, so that the detrimental impact of an increase in the building coverage (i.e. new developments) can be effectively mitigated by a suitable location of the buildings

(Bruwier et al., 2018).

## 4. Conclusion

In this study, previous research on the influence of the urban form on river flooding (Bruwier et al., 2018) was extended to the case of urban pluvial flooding. We have considered 2000 synthetic arrangements of buildings, characterized by nine urban parameters (typical street orientation, curvature, length and width, mean parcel area, building setbacks, ...), and two different terrain slopes. For each of them, we computed surface flow variables using a validated hydro-inundation model forced by uniform rainfall input corresponding to design storms of various return periods. Our results show the following:

- variations in the urban forms has generally a more limited effect on the peak values of stored volume in the urban district and on the outflow discharge compared to changes in the storm return period or in the terrain slope;
- in contrast, a strong influence of the urban form was found on the mean water depths in the urban area;
- the influence of the urban form is magnified in the case of more extreme rainfall events, which hints at a growing importance of flood-sensitive urban planning as an adaptation to climate change;
- based on statistical analysis, we highlighted the overwhelming influence of the building coverage compared to other urban parameters;
- the distance between adjacent buildings is another influencing parameter, but to a lesser extent.

From the perspective of urban planning, the strongly dominating influence of the building coverage seems to hamper the compensation of an increasing building coverage (i.e. urban development) by means of a more “flood-sensitive” arrangement of the buildings (e.g. with higher lateral setbacks), since the latter effect remains by far smaller than the former one. This result obtained here for pluvial flooding differs from earlier results obtained in the context of river flooding (Bruwier et al., 2018). Moreover, these conclusions appear robust with respect to changes in the terrain slope or in the rainfall intensity.

This study is the first one to date to analyse systematically the influence of the urban form on urban pluvial flooding. Nonetheless, given the high complexity of the actual interactions between urban systems and flow processes, our work presents a number of limitations, which should be further analysed in future research to pave the way for more flood-resilient urban planning. This includes an improved representation of urban drainage systems, land-use heterogeneity (parks, gardens ...), real-world topography (e.g. sinks), obstacles (Mignot et al., 2013), rooftops connectivity, and local water management devices (water tanks, green roofs, storm basin ...), which all have a substantial influence on urban pluvial flooding.

#### Authors contribution

P.A. and B.D. designed the study and supervised the research. A.M. operated the urban procedural model. M.B. and P.A. upgraded the hydro-inundation model. C.M. and M.B. conducted the computations and analysed the results. C.M. wrote the initial draft manuscript, which was substantially edited by M.B. and B.D. S.E., M.P. and J.T. provided expertise and feedback.

#### Declaration of Competing Interest

The authors declare that they have no known competing financial interests or personal relationships that could have appeared to influence the work reported in this paper.

#### Acknowledgements

The Authors gratefully acknowledge the group of Prof. Daniel Aliaga at Purdue University (USA) for permitting the use of the procedural model. The Authors also wish to thank Gilles Giraudet who, at an early stage of the research, conducted preliminary numerical simulations. This research was partly funded through the ARC grant for Concerted Research Actions, financed by the Wallonia-Brussels Federation.

#### Appendix A. Supplementary data

Supplementary data to this article can be found online at <https://doi.org/10.1016/j.jhydrol.2019.124493>.

#### References

- Ahiablame, L., Shakya, R., 2016. Modeling flood reduction effects of low impact development at a watershed scale. *J. Environ. Manage.* 171, 81–91.
- Arrault, A., Finaud-Guyot, P., Archambeau, P., Bruwier, M., Ercicum, S., Piroton, M., Dewals, B., 2016. Hydrodynamics of long-duration urban floods: experiments and numerical modelling. *Nat. Hazards Earth Syst. Sci.* 16, 1413–1429.
- Bazin, P.-H., Nakagawa, H., Kawaike, K., Paquier, A., Mignot, E., 2014. Modeling flow exchanges between a street and an underground drainage pipe during urban floods. *J. Hydraul. Eng.* 140.
- Brown, J.D., Spencer, T., Moeller, I., 2007. Modeling Storm Surge Flooding of an Urban Area with Particular Reference to Modeling Uncertainties: A Case Study of Canvey Island. Water Resources Research, United Kingdom, pp. 43.
- Bruwier, M., Archambeau, P., Ercicum, S., Piroton, M., Dewals, B., 2017a. Shallow-water models with anisotropic porosity and merging for flood modelling on Cartesian grids. *J. Hydrol.* 554, 693–709.
- Bruwier, M., Ercicum, S., Archambeau, P., Piroton, M., Dewals, B., 2017b. Discussion of “computing flooding of crossroads with obstacles using a 2D numerical model” by P.-H. Bazin, E. Mignot and A. Paquier. *J. Hydr. Res.* 55, 737–741.
- Bruwier, M., Mustafa, A., Aliaga, D.G., Archambeau, P., Ercicum, S., Nishida, G., Zhang, X., Piroton, M., Teller, J., Dewals, B., 2018. Influence of urban pattern on inundation flow in floodplains of lowland rivers. *Sci. Total Environ.* 622–623, 446–458.
- Cea, L., Garrido, M., Puertas, J., 2010. Experimental validation of two-dimensional depth-averaged models for forecasting rainfall-runoff from precipitation data in urban areas. *J. Hydrol.* 382, 88–102.
- Chang, T.-J., Wang, C.-H., Chen, A.S., 2015. A novel approach to model dynamic flow interactions between storm sewer system and overland surface for different land covers in urban areas. *J. Hydrol.* 524, 662–679.
- Chen, A.S., Djordjevic, S., Leandro, J., Savić, D., 2007. The urban inundation model with bidirectional flow interaction between 2D overland surface and 1D sewer networks. *NOVATECH 2007*.
- Chen, P.-Y., Tung, C.-P., Li, Y.-H., 2017. Low impact development planning and adaptation decision-making under climate change for a community against pluvial flooding. *Water (Switzerland)* 9.
- Chen, Y., Zhou, H., Zhang, H., Du, G., Zhou, J., 2015. Urban flood risk warning under rapid urbanization. *Environ. Res.* 139, 3–10.
- Djordjević, S., Prodanović, D., Maksimović, Č., Ivetić, M., Savić, D., 2005. SIPSON – simulation of interaction between pipe flow and surface overland flow in networks. *Water Sci. Technol.* 52, 275–283.
- Elboshy, B., Kanae, S., Gamaleldin, M., Ayad, H., Osaragi, T., Elbarki, W., 2019. A framework for pluvial flood risk assessment in Alexandria considering the coping capacity. *Environ. Syst. Dec.* 39, 77–94.
- Fernández-Pato, J., Caviedes-Voullième, D., García-Navarro, P., 2016. Rainfall/runoff simulation with 2D full shallow water equations: sensitivity analysis and calibration of infiltration parameters. *J. Hydrol.* 536, 496–513.
- Fewtrell, T.J., Duncan, A., Sampson, C.C., Neal, J.C., Bates, P.D., 2011. Benchmarking urban flood models of varying complexity and scale using high resolution terrestrial LiDAR data. *Phys. Chem. Earth* 36, 281–291.
- Fletcher, T.D., Andrieu, H., Hamel, P., 2013. Understanding, management and modelling of urban hydrology and its consequences for receiving waters: a state of the art. *Adv. Water Resour.* 51, 261–279.
- Gaines, J.M., 2016. Flooding: water potential. *Nature* 531, S54–S55.
- Guinot, V., Sanders, B.F., Schubert, J.E., 2017. Dual integral porosity shallow water model for urban flood modelling. *Adv. Water Resour.* 103, 16–31.
- Hosseinzadehtalaei, P., Tabari, H., Willems, P., 2018. Precipitation intensity-duration-frequency curves for central Belgium with an ensemble of EURO-CORDEX simulations, and associated uncertainties. *Atmos. Res.* 200, 1–12.
- Hsu, M.H., Chen, S.H., Chang, T.J., 2000. Inundation simulation for urban drainage basin with storm sewer system. *J. Hydrol.* 234, 21–37.
- Huang, Q., Wang, J., Li, M., Fei, M., Dong, J., 2017. Modeling the influence of urbanization on urban pluvial flooding: a scenario-based case study in Shanghai, China. *Nat. Hazards* 87, 1035–1055.
- JBA Consulting. 2016. Pluvial Flood Mapping for Flanders. Pilot Project Report.
- Skougaard Kaspersen, P., Hoegh Ravn, N., Arnbjerg-Nielsen, K., Madsen, H., Drews, M., 2017. Comparison of the impacts of urban development and climate change on exposing European cities to pluvial flooding. *Hydrol. Earth Syst. Sci.* 21, 4131–4147.
- Kreibich, H., Thaler, T., Glade, T., Molinari, D., 2019. Preface: Damage of natural hazards: assessment and mitigation. *Nat. Hazards Earth Syst. Sci.* 19, 551–554.
- Leandro, J., Chen, A.S., Djordjević, S., Savić, D.A., 2009. Comparison of 1D/1D and 1D/2D coupled (sewer/surface) hydraulic models for urban flood simulation. *J. Hydraul. Eng.* 135, 495–504.
- Leandro, J., Martins, R., 2016. A methodology for linking 2D overland flow models with the sewer network model SWMM 5.1 based on dynamic link libraries. *Water Sci. Technol.* 73, 3017–3026.
- Leandro, J., Schumann, A., Pfister, A., 2016. A step towards considering the spatial heterogeneity of urban key features in urban hydrology flood modelling. *J. Hydrol.* 535, 356–365.
- Löwe, R., Urich, C., Domingo, N. Sto., Mark, O., Deletic, A., Arnbjerg-Nielsen, K., 2017. Assessment of urban pluvial flood risk and efficiency of adaptation options through simulations – a new generation of urban planning tools. *J. Hydrol.* 550, 355–367.
- Martins, R., Kesserwani, G., Rubinato, M., Lee, S., Leandro, J., Djordjević, S., Shucksmith, J.D., 2017. Validation of 2D shock capturing flood models around a surcharging manhole. *Urban Water J.* 14, 892–899.
- Mignot, E., Paquier, A., Haider, S., 2006. Modeling floods in a dense urban area using 2D shallow water equations. *J. Hydrol.* 327, 186–199.

- Mignot, E., Zeng, C., Dominguez, G., Li, C.-W., Rivière, N., Bazin, P.-H., 2013. Impact of topographic obstacles on the discharge distribution in open-channel bifurcations. *J. Hydrol.* 494, 10–19.
- Miller, J.D., Hutchins, M., 2017. The impacts of urbanisation and climate change on urban flooding and urban water quality: A review of the evidence concerning the United Kingdom. *J. Hydrol.: Reg. Stud.* 12, 345–362.
- Muis, S., Güneralp, B., Jongman, B., Aerts, J.C.J.H., Ward, P.J., 2015. Flood risk and adaptation strategies under climate change and urban expansion: a probabilistic analysis using global data. *Sci. Total Environ.* 538, 445–457.
- Mustafa, A., Wei Zhang, X., Aliaga, D.G., Bruwier, M., Nishida, G., Dewals, B., Ercicum, S., Archambeau, P., Pirotton, M., Teller, J., 2018. Procedural generation of flood-sensitive urban layouts. *Environ. Plann. B: Urban Anal. City Sci.*
- Qin, H.-P., Li, Z.-X., Fu, G., 2013. The effects of low impact development on urban flooding under different rainfall characteristics. *J. Environ. Manage.* 129, 577–585.
- Russo, B., Sunyer, D., Velasco, M., Djordjević, S., 2015. Analysis of extreme flooding events through a calibrated 1D/2D coupled model: the case of Barcelona (Spain). *J. Hydroinf.* 17, 473–491.
- Salvadore, E., Bronders, J., Batelaan, O., 2015. Hydrological modelling of urbanized catchments: a review and future directions. *J. Hydrol.* 529, 62–81.
- Sampson, C.C., Bates, P.D., Neal, J.C., Horritt, M.S., 2013. An automated routing methodology to enable direct rainfall in high resolution shallow water models. *Hydrol. Process.* 27, 467–476.
- Sanders, B.F., Schubert, J.E., Gallegos, H.A., 2008. Integral formulation of shallow-water equations with anisotropic porosity for urban flood modeling. *J. Hydrol.* 362, 19–38.
- Schmitt, T.G., Thomas, M., Ettrich, N., 2004. Analysis and modeling of flooding in urban drainage systems. *J. Hydrol.* 299, 300–311.
- Seyoum, S.D., Vojinovic, Z., Price, R.K., Weesakul, S., 2012. Coupled 1D and noninertia 2D flood inundation model for simulation of urban flooding. *J. Hydraul. Eng.* 138, 23–34.
- Yin, J., Jing, Y., Yu, D., Ye, M., Yang, Y., Liao, B., 2019. A vulnerability assessment of urban emergency in schools of Shanghai. *Sustainability (Switzerland)* 11.
- Yin, J., Ye, M., Yin, Z., Xu, S., 2015. A review of advances in urban flood risk analysis over China. *Stoch. Env. Res. Risk Assess.* 29, 1063–1070.
- Yin, J., Yu, D., Yin, Z., Liu, M., He, Q., 2016. Evaluating the impact and risk of pluvial flash flood on intra-urban road network: a case study in the city center of Shanghai, China. *J. Hydrol.* 537, 138–145.
- Yu, D., Coulthard, T.J., 2015. Evaluating the importance of catchment hydrological parameters for urban surface water flood modelling using a simple hydro-inundation model. *J. Hydrol.* 524, 385–400.
- Zhou, Q., Mikkelsen, P.S., Halsnæs, K., Arnbjerg-Nielsen, K., 2012. Framework for economic pluvial flood risk assessment considering climate change effects and adaptation benefits. *J. Hydrol.* 414–415, 539–549.